TECTONICS, VOL. 12, NO. 3, PAGES 688-702, JUNE 1993

PALEOMAGNETIC CONSTRAINTS ON THE INITIATION OF UPLIFT ON THE SANTA SUSANA FAULT, WESTERN TRANSVERSE RANGES, CALIFORNIA

Shaul Levi
College of Oceanography, Oregon State University, Corvallis
Robert S. Yeats
Department of Geosciences, Oregon State University, Corvallis

Abstract. The Plio-Pleistocene nonmarine Saugus Formation is widely exposed in the east Ventura basin and the northern San Fernando Valley, north and south of the Santa Susana fault. In the east Ventura basin, the Saugus is overlain by the Pacoima Formation. Magnetostratigraphy of the fine-grained Saugus and Pacoima strata and the presence of the 0.76 Ma Bishop ash are used to calculate their average sedimentation rates: 0.9 km/m.y. in the east Ventura basin and 1.1 km/m.y. in the northern San Fernando Valley. Extrapolation of the Saugus and Pacoima sedimentation rates shows that they were deposited from about 2.3 to 0.5 Ma both north and south of the Santa Susana fault. The shift from remote to locally derived clasts marks the initiation of uplift of the Santa Susana Mountains. The extrapolated age of this boundary is about 0.7–0.6 Ma.

INTRODUCTION

The Santa Susana fault is part of a discontinuous reverse-fault system, north side up, extending east from Santa Barbara to the San Jacinto fault near San Bernardino (Figure 1). Other faults in this system include the Red Mountain, San Cayetano, San Fernando, Sierra Madre, and Cucamonga faults. The 1971 San Fernando earthquake (M = 6.4) and smaller earthquakes on the Red Mountain, San Cayetano, and Santa Susana faults are evidence that the faults are seismically active and constitute an earthquake risk [Yerkes and Lee, 1979; Lee et al., 1979; Yeats et al., 1987].

The times of initiation and the rates of displacement on reverse faults in this zone are difficult to determine because, in most cases, rocks of the hanging wall are much older than the time of faulting. However, the Santa Susana fault cuts across the Neogene Ventura basin, where Pliocene and Pleistocene strata are preserved in both the hanging wall and footwall blocks. The Santa Susana Mountains are being uplifted by ramping on the Santa Susana fault, and the age of appearance of detritus from this newly eroded local source is a clue to the age of initiation of faulting [Saul, 1975; Yeats, 1979]. Locally derived detritus appears in the late Quaternary sequence of both the hanging wall and footwall blocks. We have dated this sequence on both sides of the fault using magnetostratigraphy, aided by the identification of an ash bed in the hanging wall sequence near Newhall, which is geochemically similar to the Bishop and Friant Tuffs [Sarna-Wojcicki et al., 1991]. From this, we determine sediment accumulation rates in this sequence on both sides of the fault and the age of initiation of movement on the Santa Susana fault.

Paper number 93TC00133.
0278-7407/93/93TC-00133$10.00

GEOLOGIC SETTING

The Santa Susana fault extends 28 km east-southeast from near the Santa Clara Valley in Ventura County to the San Fernando Valley in Los Angeles County (Figure 2). The fault ruptured the southwestern edge of a thick trough sequence of Miocene to Pleistocene sediments. The thick sequence of the Santa Susana Mountains overrides a coeval thin sequence of the Oak Ridge-Simi Hills structural shelf [Yeats, 1987] (R. S. Yeats et al., Late Cenozoic tectonics of the east Ventura basin, Transverse Ranges, California, submitted to Bulletin of the American Association of Petroleum Geologists, 1992; hereinafter referred to as Yeats et al., submitted manuscrit, 1992). The fault dies out to the northwest near the Santa Clara Valley, where strata of Miocene and Pliocene age are continuous across the westward projection of the fault [Yeats, 1987]. The fault contains two left-stepping lateral ramps, one at Gillibrand Canyon (GC, Figure 2) in the central part of the fault, and one farther east at the northwest edge of the San Fernando Valley (SF, Figure 2). East of the San Fernando lateral ramp, the fault breaks up into several strands, at least one of which moved during the 1971 San Fernando earthquake.

The Modelo Formation (middle-late Miocene), Towsley Formation (latest Miocene-earliest Pliocene), and Fernando Formation (Pliocene) were influenced by the old depositional hinge line, northeast side down, and thus they predate the Santa Susana fault. The Torrey and Frew reverse faults cut the Fernando Formation and are overlain unconformably by the Quaternary Saugus Formation [Yeats, 1979, 1987]. Absence of scarp-derived detritus from these pre-Saugus faults suggests that they were not accompanied by extensive subaerial uplift of their hanging walls. The Saugus Formation [Kew, 1924; Winterer and Durham, 1962], the main subject of this magnetostratigraphic study, occupies the center of the east Ventura basin where it is conformable with underlying Pliocene strata. South of the Santa Susana fault, the Saugus occurs in discontinuous patches that unconformably overlie faulted strata as old as Eocene that are overridden by the Santa Susana fault [Yeats, 1987].

Near the center of the east Ventura basin on the south side of the Santa Clara River valley, southwest of the Magic Mountain Amusement Park (Figure 3), the Saugus Formation rests conformably on sandstone, siltstone, and conglomerate of the marine Pliocene Pico Formation of Winterer and Durham [1962]. We follow current practice in calling the Pico strata the Fernando Formation (compare Jennings and Strand [1969] and discussion of Yeats et al. [submitted manuscript, 1992]). Winterer and Durham [1962] included in the Saugus brown, reddish-brown, and tan sandstone and conglomerate, reddish-brown mudstone, and greenish-gray sandstone, all of which are deformed. The Saugus is overlain by generally flat-lying terrace deposits similar to, but somewhat more consolidated than, the modern Santa Clara River alluvium.

Treiman [1986] found an angular unconformity within the sequence mapped by Winterer and Durham [1962] as Saugus. Below the unconformity, Saugus clasts are predominantly derived from highlands to the east, including the San Gabriel Mountains. The upper part of the Saugus contains an ash

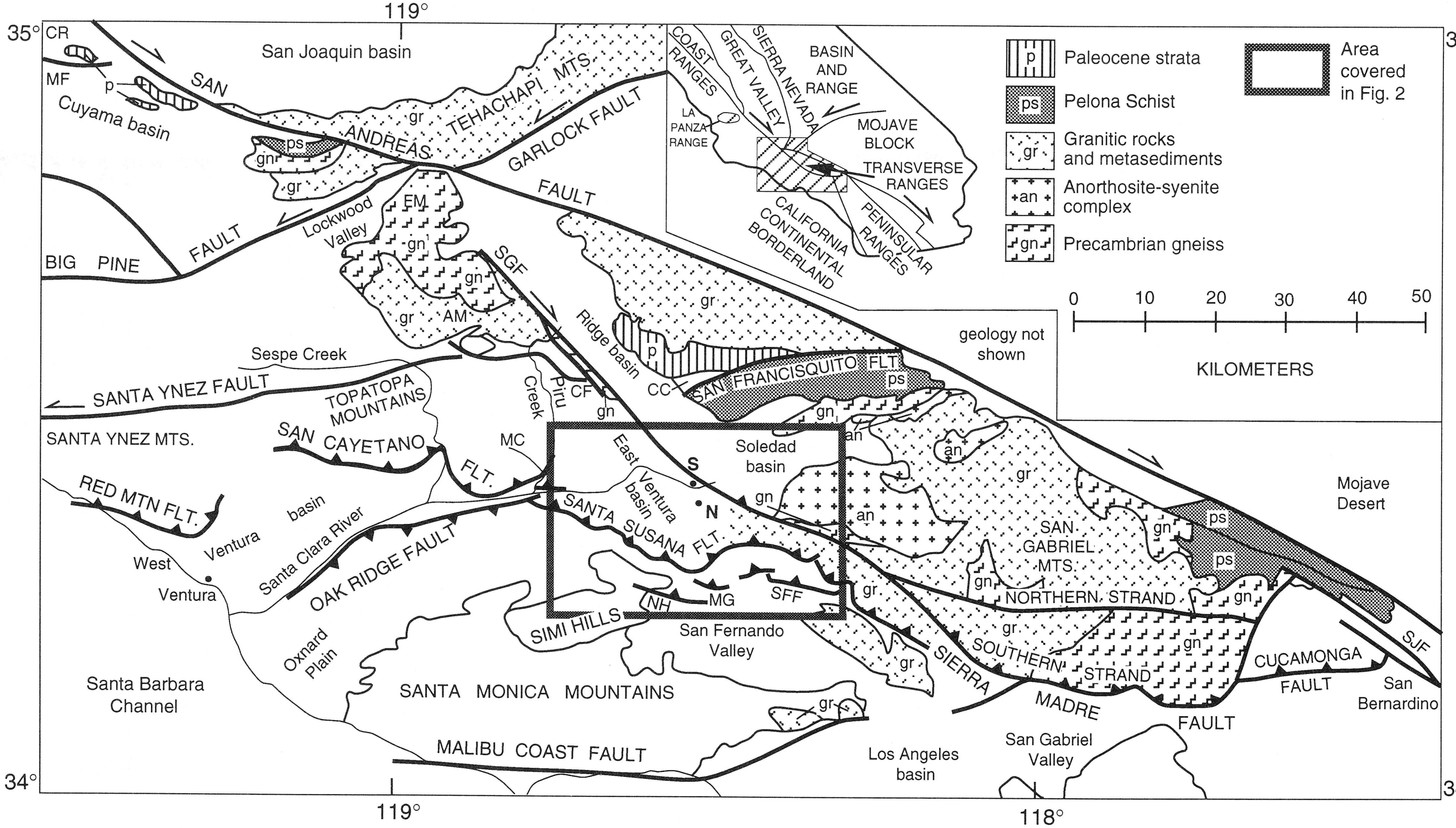

Fig. 1. Index map of east Ventura basin and Santa Susana fault. Base map is from Jennings [1975]; basement geology of San Gabriel Mountains is from Ehlig [1975]. Abbreviations are AM, Alamo Mountain; CC, Canton Creek; CF, Canton fault; CR, Caliente Range; FM, Frazier Mountain; MC, Modelo Canyon; MF, Morales fault; MG, Mission-Granada Hills fault; N, Newhall; NH, Northridge Hills fault; S, Saugus; SFF, San Fernando fault; and SGF, San Gabriel fault. Flt is fault.

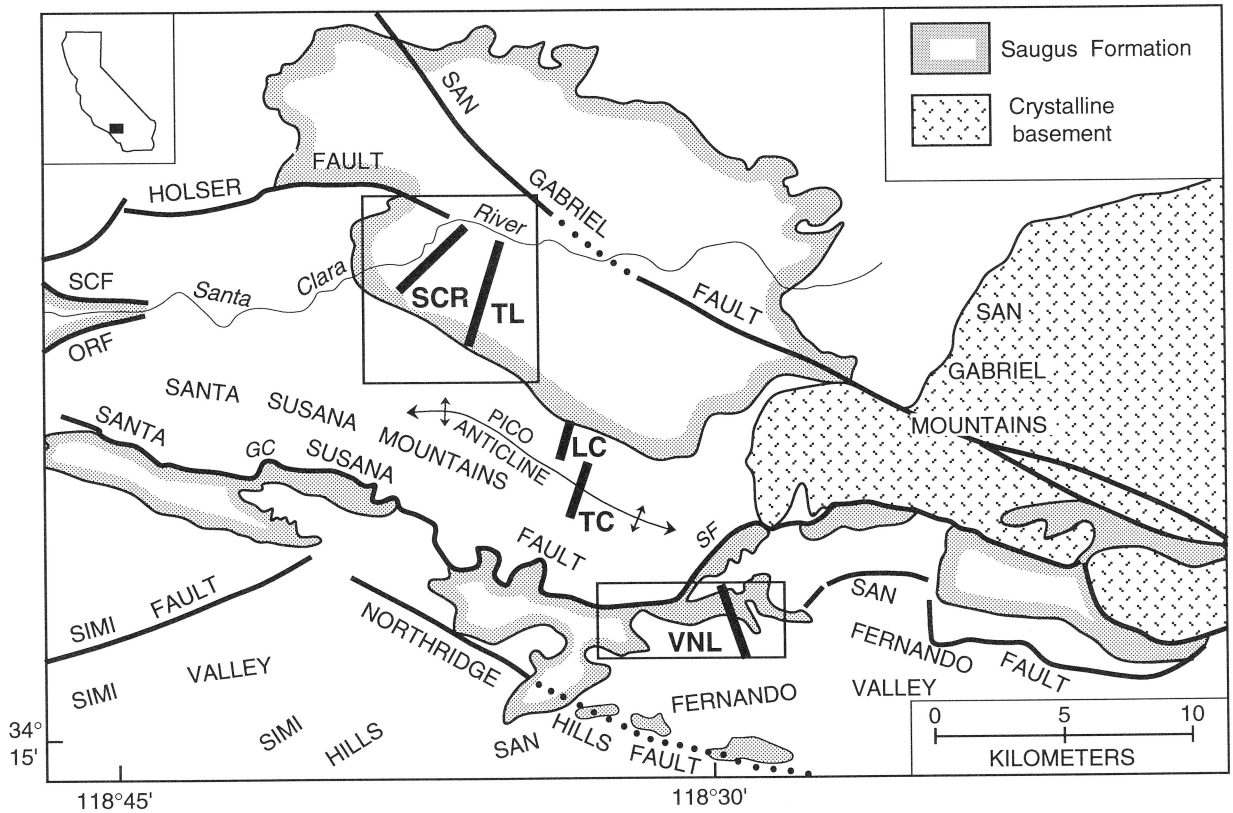

Fig. 2. Location of Saugus outcrops in the study area; also shown are several Quaternary faults with known potential for ground rupture. The rectangles enclose the Saugus sections analyzed and discussed in this paper: Santa Clara River (SCR), Transmission Line (TL), and Van Norman Lake (VNL). Older strata from the Modelo, Towsley, and Fernando formations, in Lyons Canyon (LC) and Towsley Canyon (TC) sections provided unsatisfactory paleomagnetic results. GC is Gillibrand Canyon lateral ramp; SF is San Fernando lateral ramp. Other abbreviations are SCF, San Cayetano fault; ORF, Oak Ridge fault. Figure adapted from map of Barrows et al. [1975].

layer which is geochemically very similar to the Bishop ash (0.76 Ma) and the Friant ash (0.62 Ma); a definite correlation to one or the other could not be made (work of A. M. Sarna-Wojcicki as discussed by Levi et al. [1986]. The strata above the unconformity contain clasts of shale, siltstone, and sandstone similar to bedrock now exposed in the Santa Susana Mountains to the south. Treiman [1986] correlated the locally derived strata to the Pacoima Formation mapped by Oakeshott [1958] northwest of the San Gabriel Mountains. J. A. Treiman (personal communication, 1991) recognized that this may not be equivalent to Oakeshott's Pacoima in the San Fernando Valley. The Pacoima-Saugus contact is exposed in a road cut adjacent to the Exxon NL&F 24 well (Figure 3), where the contact may be conformable. Northwest of this well, the strata become conformable and more lithologically alike (J. A. Treiman, personal communication, 1992). We projected the contact along strike, but the strata above the contact are only questionably mapped as Pacoima Formation [Treiman, 1986; J. A. Treiman, written communications, 1991]. The Pacoima includes strata mapped by Winterer and Durham [1962] as terrace deposits, but the Pacoima dips to the northeast and is undoubtedly older. In the Magic Mountain area (Figure 3) the upper part of the Saugus and the Pacoima formations dip to the northeast. At the northern end of the Pacoima outcrop, west of Magic Mountain Amusement Park, the Pacoima is in fault contact with Saugus and terrace deposits. This fault may be the eastern projection of a strand of the Holser fault (Figure 2), although the Holser fault may project farther north.

South of the Santa Susana fault in the San Fernando Valley, the north-dipping Pliocene-Pleistocene sequence west of Van Norman Lake was mapped by Oakeshott [1958], and it includes the fossiliferous marine sandstone, mudstone, and conglomerate of his Pico Formation (Fernando Formation of this paper); the nonmarine and brackish-water sandstone, mudstone, and conglomerate with thin limestone beds which he called the Sunshine Ranch Member of the Pico Formation; and the nonmarine light-colored conglomerate and sandstone of the Saugus Formation (Figure 4). Barrows et al. [1975] and Saul [1975] included the Sunshine Ranch Member in the Saugus Formation rather than the Pico Formation, although they, like Oakeshott, regarded it as Pliocene in age. They noted that the Sunshine Ranch Member is typically greenish- to reddish-gray siltstone and sandstone with coarser-grained sandstone and less common layers of conglomerate, whereas the overlying member of the Saugus Formation is mostly sandstone and conglomerate with a source area to the north in the San Gabriel Mountains. Barrows et al. [1975] and Saul

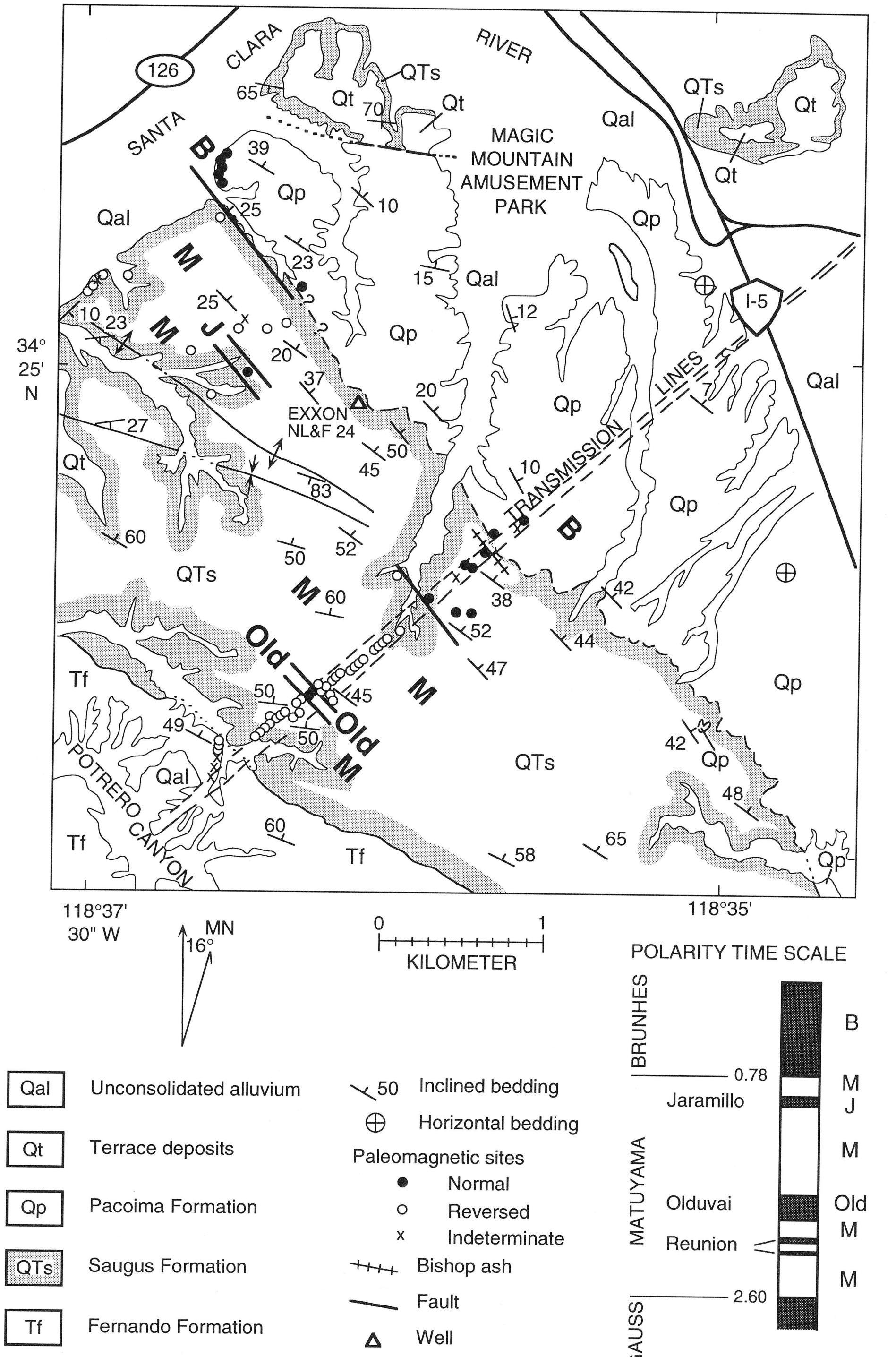

Fig. 3. Simplified geologic map of the Magic Mountain area, redrawn from maps of Winterer and Durham [1962] and Treiman [1986]. Paleomagnetic sampling sites at the TL and SCR sections are shown as closed (normal) and open (reversed) circles and crosses (unstable). Heavy line segments represent inferred polarity boundaries. Abbreviations are B, Brunhes; M, Matuyama; Old, Olduvai; and J, Jaramillo.

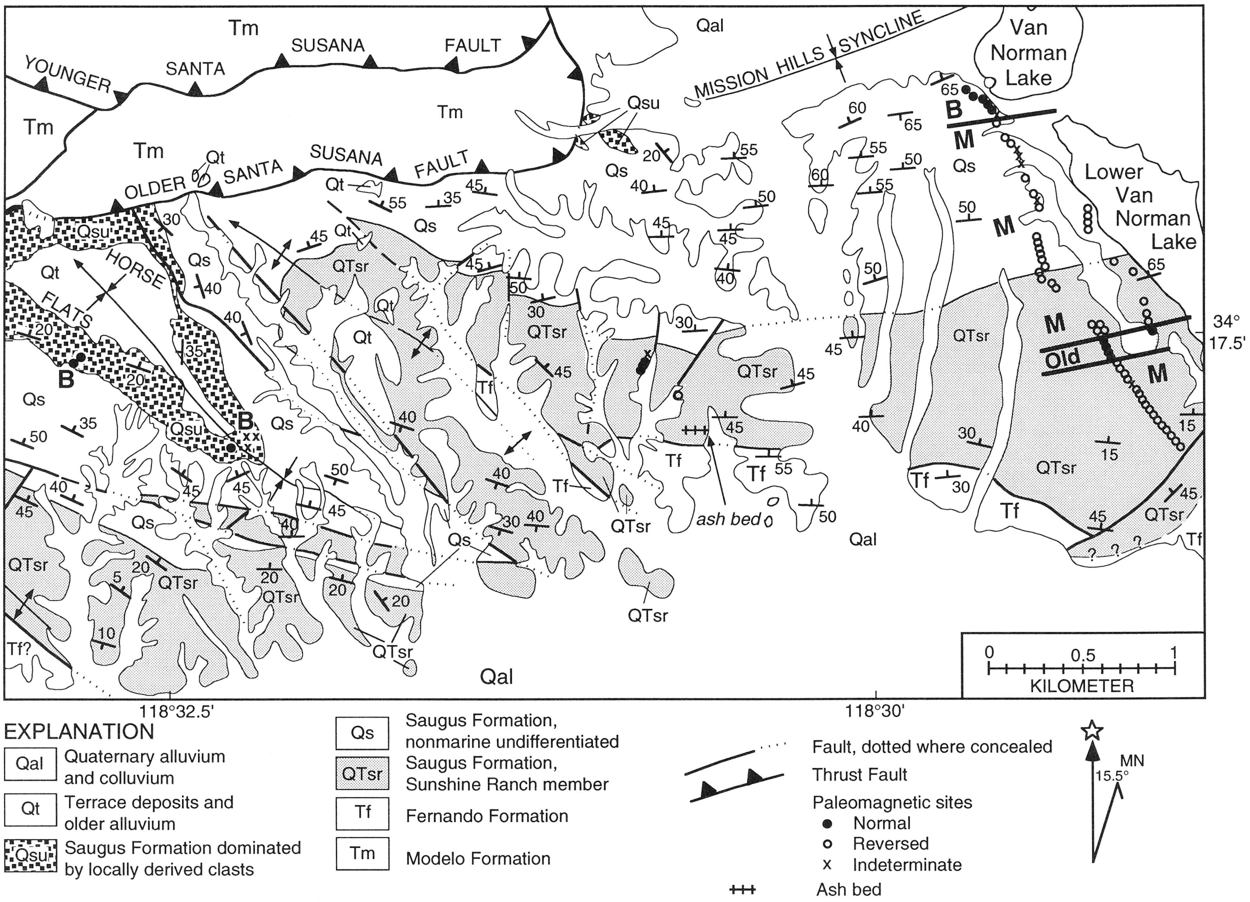

Fig. 4. Simplified geologic map of the Horse Flats and Van Norman Lake reservoir area redrawn from map of Barrows et al. [1975]. Paleomagnetic sampling sites are shown as closed (normal) and open (reversed) circles and crosses (unstable and overprinted). Heavy line segments represent inferred polarity boundaries. Abbreviations are B, Brunhes; M, Matuyama; and Old, Olduvai.

[1975] mapped these formations westward to the Santa Susana fault area, where they found that the Saugus is overlain unconformably by terrace deposits which are themselves downwarped into a broad syncline at Horse Flats (Figure 4).

At Horse Flats, Saul [1979] mapped a distinct uppermost member of the Saugus Formation, in which coarse clastic layers are dominated by clasts of calcareous sandstone and porcelaneous shale, rocks common in the Santa Susana Mountains to the north. The basal contact of this unit is gradational with the rest of the Saugus. In the upper 10 to 20 m of the underlying Saugus, the clast lithologies change upward from remotely derived igneous and metamorphic rocks to locally derived sedimentary rocks; the contact is drawn where the clasts are almost exclusively locally derived. Saul [1975, 1979] recognized that this change in clast lithology indicated the initiation of uplift of the Santa Susana Mountains to the north. Uplift shielded the Horse Flats area from the San Gabriel source region which had previously provided most of the clasts. The uppermost Saugus member does not appear to be present at Van Norman Lake, possibly because of its location east of the Santa Susana Mountains.

The homoclinal structure of the Saugus Formation near Van Norman Lake continues westward toward the Santa Susana fault, where bedding strike changes to west-northwest, and broad west-northwest-trending folds are found plunging gently toward the Santa Susana fault (Figure 4). Horse Flats is the site of a broad constructional surface underlain by older alluvium which appears to be warped by the Horse Flats syncline. The section is cut by many high-angle faults of small displacement, and detailed bed-to-bed correlation of the Saugus Formation between Van Norman Lake and Horse Flats is not possible. However, a general correlation is possible using (1) the top of the Sunshine Ranch Member and (2)

TABLE 1. Saugus Formation Site Inventory

Saugus Locality	Number of Sites, Sampled	Number of Sites, Polarity	Number of Sites, Direction	Number of Specimens Used/Measured
TL	48	44	26	182/196
SCR	21	19	16	90/94
VNL	72	66	51	304/327
HF	11	8	6	35/42
Total	152	137	99	611/659

TL is Transmission Line; SCR is Santa Clara River; VNL is Van Norman Lake; HF is Horse Flats.

the boundary between the locally and remotely derived clasts of the continental Saugus Formation.

Older alluvium rests unconformably on the southern strand of the Santa Susana fault, leading Saul [1975, 1979] to conclude that the Santa Susana fault has been inactive since the middle Pleistocene. However, Lant [1977] and Yeats [1987] showed that the southern strand has been folded and displaced by a younger strand that reaches the surface farther north within the Santa Susana Mountains (Younger Santa Susana fault of Figure 4).

FIELD AND SAMPLING PROCEDURES

In the hanging wall north of the Santa Susana fault the Fernando and Saugus formations were extensively sampled for paleomagnetism in the north limb of the Pico anticline, south of the Holser and San Gabriel faults. Five Fernando Formation sites were sampled in the north limb of the Pico anticline in Lyons Canyon (Figure 2), as well as 16 sites from the Towsley and Modelo formations, straddling the Pico anticline in Towsley Canyon (Figure 2). In the Magic Mountain Amusement Park area, where the nonmarine Saugus is more than 1.5 km thick, we assembled a composite section along the Santa Clara River (SCR) and along a trench paralleling a set of transmission lines (TL) (Figure 3). In this area, it is possible to make general (not bed to bed) correlation between the TL and SCR sections [Winterer and Durham, 1962] (Figure 3). The TL section is unfaulted, and the beds dip homoclinally about 50° to the north-northeast. The SCR section exposes beds which dip more gently (20°–30°) to the northeast.

In the footwall south of the Santa Susana fault, 72 Saugus sites were sampled in an approximately 2-km-thick section along the west side of the Van Norman Lake (VNL) Reservoir, in the northwest corner of the San Fernando valley (Figure 2). In this area (just west of the Golden State Freeway), the Saugus is homoclinal, dipping northward 20°–60°, and it comprises both the brackish-water Sunshine Ranch and the overlying non marine members. Eleven additional sites were sampled in the area west of the Van Norman Reservoir: four sites along Nugent Street (middle of Figure 4), one site at a building excavation along Andasol Avenue (reverse site in the middle of Figure 4), four sites along Reseda Boulevard on the way to Horse Flats, and two sites at Horse Flats near the intersection of Braemore Road and Bowmore Avenue (clusters of four and two upper Saugus sites, respectively, at left one fourth of Figure 4).

Sites for paleomagnetism were selected at the finer-grained sedimentary interbeds of mudstone, siltstone, sandy siltstone, and silty sandstone, typically 0.5 to 5 m thick, and usually sandwiched between much thicker beds of coarser sandstone and conglomerate. At each site, digging was usually required to expose less-weathered sediment for sampling. The samples were oriented prior to removing them from the outcrop; orientation was usually done by scribing a north arrow on a freshly carved and leveled horizontal surface. In this manner, three samples were usually obtained from each site. In the laboratory, each sample was releveled in a plaster of paris cast, and two specimens for paleomagnetic measurements were cut or drilled from each hand sample.

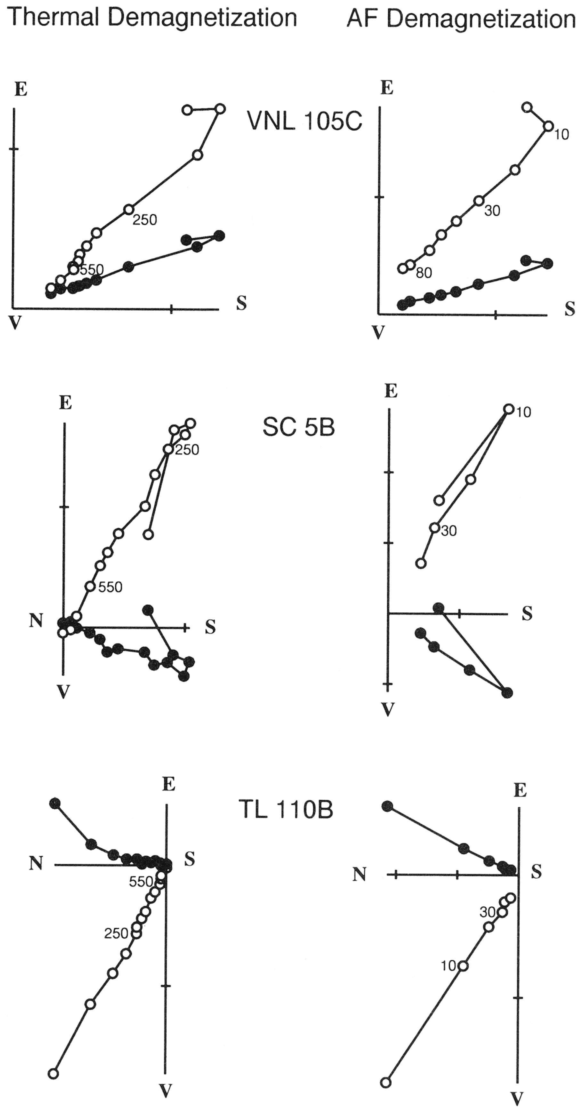

Fig. 5. Examples of similar behavior of alternating fields (AF) and thermal demagnetizations for specimens from the same hand sample, plotted in geographic coordinates after structural correction. Solid circles represent remanence endpoints projected onto the horizontal plane; open circles, endpoints projected onto a vertical plane. The AF levels are in millitesla (mT); temperatures are in degrees centigrade (°C). Tick-mark separations are 10^{-2} A/M.

STABILITY OF THE REMANENCE

The sites from the marine Modelo and Towsley formations in Towsley Canyon, as well as sites from the marine Fernando (Pico) Formation at Lyons Canyon and from near the Santa Clara River are pervasively overprinted by the present magnetic field, and we were unable to recover the primary remanence, using both alternating fields (AF) and thermal demagnetization methods. Only three Fernando sites immediately below the Fernando/Saugus boundary at the base of

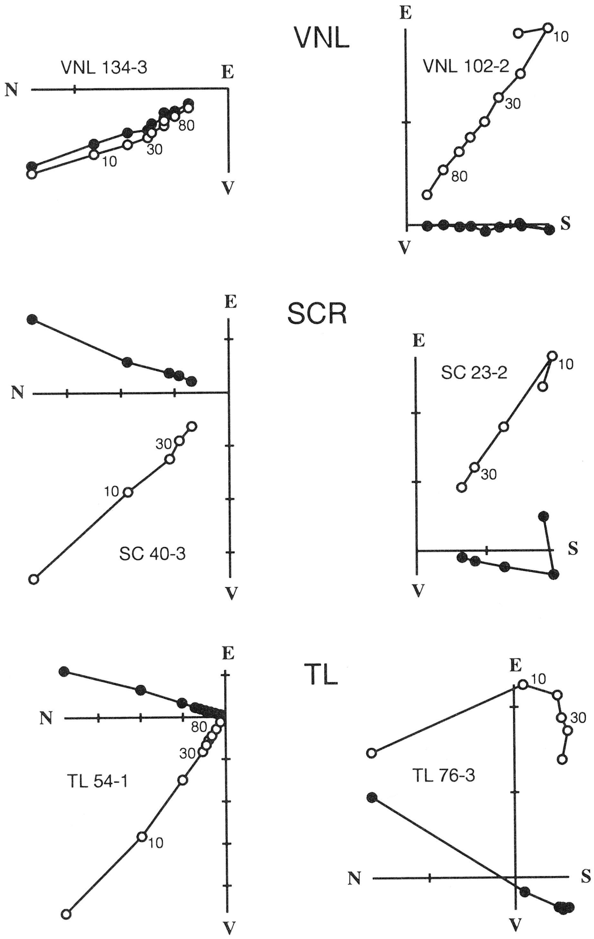

Fig. 6. Examples of alternating fields (AF) demagnetizations of one normal and one reverse specimen from Van Norman Lake (VNL), Santa Clara River (SCR), and Transmission Line (TL) sections, plotted in geographic coordinates after structural correction. Solid circles represent remanence endpoints projected onto the horizontal plane; open circles, endpoints projected onto a vertical plane. The AF levels are in millitesla (mT). Tick-mark separations are 10^{-2} A/M.

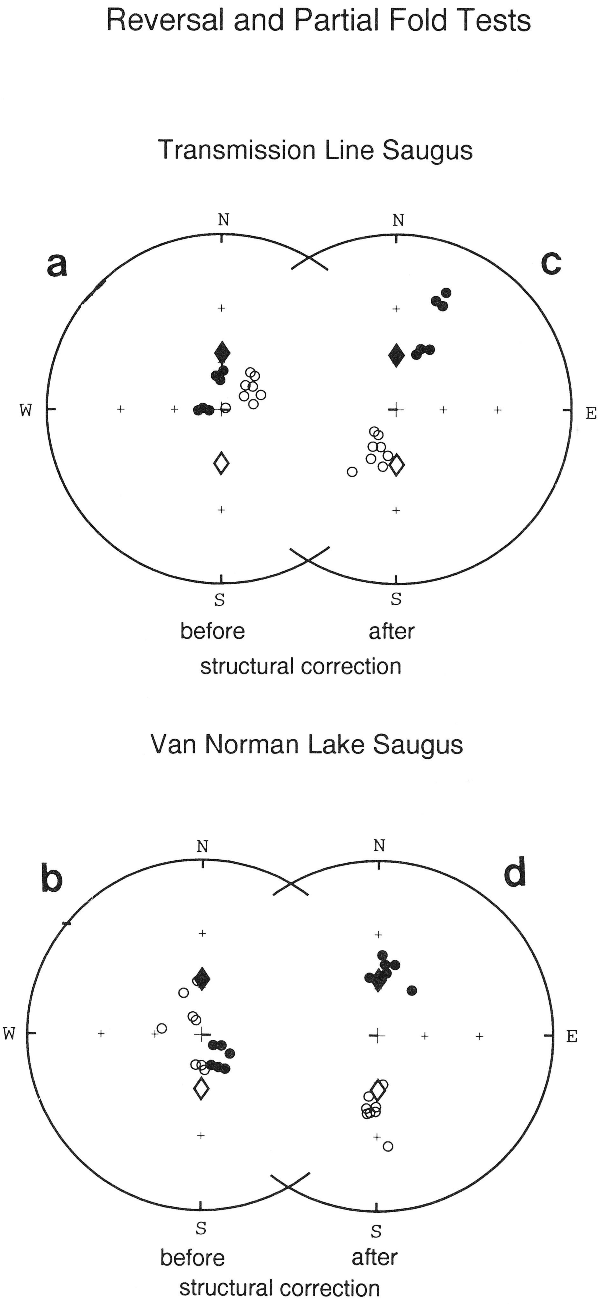

Fig. 7. Site mean directions of normal Matuyama (Olduvai) sites and a similar number of bracketing reverse sites in the Transmission Line and Van Norman Lake sections before and after structural corrections. Diamonds represent the Plio-Pleistocene geocentric axial dipole direction. Solid symbols represent lower hemisphere directions; open symbols, upper hemisphere directions. Note that prior to structural correction the results are incompatible with the geocentric axial dipole inclination and would fail the reversal test. The structurally corrected directions satisfy both the reversal and fold tests. (The three normal Transmission Line sites with structurally corrected shallow inclinations belong to TL 57, TL 59, and TL 60, which are transitional between normal and reverse; see Table 2.)

the TL section (Figure 3) have reverse polarity. In contrast, the fine-grained, nonmarine Saugus strata retain, for the most part, a stable remanence (Table 1). At present, we can only speculate that mild reheating due to burial destroyed the primary remanence and is the cause for the remanence instability of the marine Modelo, Towsley, and Fernando formations, as compared with the relatively stable nonmarine Saugus.

For the Saugus Formation, thermal and AF demagnetization were, in general, equally effective at removing secondary overprints (Figure 5). AF demagnetization was chosen as the primary "cleaning" method for this study. At least two specimens from each site were demagnetized in progressively increasing alternating fields up to between 40 and 100 mT (millitesla), to isolate the characteristic remanence and to determine the blanket alternating fields for demagnetizing the remaining specimens at each site. At least four blanket AF

TABLE 2. Transmission Line Section: Site Mean Paleomagnetic Results

Site	N/n	D, deg	I, deg	k	α_{95}, deg	Demag, mT	Bedding Strike/Dip
			Saugus Formation				
TL116	3/4	normal					
TL114		unstable					
TL112	4/6	normal					
TL110	6/6	17	63	360	4	20–40	
TL108	4/6	normal					
TL106	6/6	8	49	31	12	20–40	326°/38°NE
TL104		unstable					313.5°/37°NE
TL103	6/6	19	41	27	13	40–80	
TL101	4/6	normal					315.5°/54°NE
TL100	6/8	9	33	26	13	30–80	306°/52°NNE
TL99	4/6	reversed					
TL94	6/6	206	−54	30	13	10–30	
TL90	6/6	reversed					308°/46°NNE
TL87	6/6	208	−58	207	5	20–40	308°/48°NE
TL86	4/8	213	−51	54	13	30–50	
TL84	6/6	190	−60	55	9	30–50	
TL82	6/6	207	−55	376	3	30–50	
TL80	6/6	193	−53	102	7	30–50	
TL78	4/4	reversed					
TL76	8/8	202	−64	400	3	20–40	
TL72	5/6	reversed					
TL70	2/4	reversed					
TL68	2/4	reversed					
TL66		unstable					
TL64	6/6	230	−45	137	6	40–60	
TL60*	15/15	24	24	83	4	50–100	308°/50°NNE
TL59*	12/12	23	18	32	8	60–100	
TL57*	12/12	20	23	49	6	60–100	
TL56	6/8	22	49	197	5	20–40	
TL55	6/6	29	47	248	4	20–40	
TL54	8/8	22	50	132	5	10–30	307°/45°NNE
TL51B	2/6	normal					
TL51	2/2	normal					
TL50	6/7	reversed					
TL30	6/8	215	−43	43	10	20–40	308°/50°NNE
TL22	10/13	212	−62	29	9	50–80	
TL21	6/6	218	−70	113	6	40–50	
TL20	6/6	reversed					
TL19	6/6	215	−70	118	6	30–50	
TL16	6/6	216	−71	105	7	40–50	
TL14	6/6	207	−70	164	5	40–60	
TL12	5/6	reversed					
TL10	5/6	reversed					
TL8	4/8	reversed?					
TL6	5/6	reversed					
TL4	6/6	220	−52	144	6	30–50	
TL3	6/6	reversed					308°/50°NNE
TL2		unstable					
TL1	5/6	224	−56	109	7	20–40	
			Fernando Formation				
P6	4/8	reversed					
P5	5/6	reversed					314°/49°NE
P4	4/8	reversed					
P3		unstable					
P2		unstable					
P1		unstable					282°/37°NE

TABLE 2. (continued)

N/n is the number of specimens used in calculations/number of specimens measured; D and I are structurally corrected declination (D) and inclination (I), rotated to horizontal using measured bedding attitude (strike/dip); k is best estimate of precision parameter of Fisher distribution; α_{95} is radius in degrees of the 95% cone of confidence about the mean direction; demag is the range of consecutive alternating fields (AF) demagnetization steps in millitesla used for obtaining the stable direction of each specimen. Site location is 34.39°N latitude, 241.40°E longitude. * sites with anomalous (transitional?) paleomagnetic directions.

levels were used to demagnetize each specimen of every site (Figure 6).

Assessment of the remanence stability of the Saugus units was made easier by the predominance of reverse polarity, which is usually more readily distinguished from present-day overprints than normal polarity remanence. Many of the reverse specimens had a superimposed normal remanence component, which was usually removed by low-temperature (< 200° C) thermal or low-field (< 20 mT) AF demagnetization, and some of the reverse specimens showed a characteristic increase of the magnetization intensity during the initial stages of demagnetization. In addition, the Saugus Formation

TABLE 3. Santa Clara River Section: Site Mean Paleomagnetic Results for Saugus Formation

Site	N/n	D, deg	I, deg	k	α_{95}, deg	Demag, mT	Bedding Strike/Dip
SC40	6/6	16	44	87	7	20–40	
SC36	6/6	21	51	169	5	20–40	
SC34	6/6	19	48	119	6	20–40	
SC32	6/6	13	52	85	7	20–40	
SC6	6/6	7	47	56	9	10–30	308.5°/32°NE
SC57	6/6	16	46	38	11	40–50	
SC20	6/6	192	−58	81	8	30–50	
SC51	4/6	reversed					
SC29	6/6	184	−49	68	8	20–40	
SC28	6/6	reversed					
SC27		unstable					319°/20°NE
SC24	6/6	223	−36	19		30–50	330°/25°NE
SC25	5/6	39	57	66	9	30–50	330°/26°NE
SC23	6/6	198	−52	96	7	20–40	330°/27°NE
SC5	6/6	208	−53	233	4	20–40	
SC16	5/6	227	−58	16	20	30–50	328°/27°NE
SC10		unstable					320°/32°NE
SC4	5/6	reversed					356°/22°NE
SC3	4/4	216	−57	148	8	20–40	
SC2	5/6	197	−64	16	20	60–100	27°/34°SE
SC1	6/6	222	−55	189	5	10–30	

See Table 2 notes for definitions of column heads. Site location is 34.42°N latitude, 241.39°E longitude.

TABLE 4. Van Norman Lake Section: Site Mean Paleomagnetic Results for Saugus Formation

Site	N/n	D, deg	I, deg	k	α_{95}, deg	Demag, mT	Bedding Strike/Dip
VNL138	5/6	356	33	94	8	30–100	264°/53°N
VNL136	6/6	353	29	146	6	30–100	257°/70°N
VNL134	5/5	335	28	47	11	30–100	
VNL132	6/6	336	31	88	7	30–100	245°/70°N
VNL130	6/6	355	40	125	6	30–100	260°/70°N
VNL128	5/6	overprinted					260°/82°N
VNL126	4/6	196	–43	63	12	30–100	263°/80°N
VNL124	6/6	reversed					250°/65°N
VNL122	4/6	reversed					244°/71°N
VNL120	6/6	overprinted					256°/73.5°N
VNL119		unstable					252°/82°N
VNL118	6/6	overprinted					255°/64°N
VNL115	4/6	177	–60	26	25	50–100	250°/56°N
VNL114	6/6	170	–24	55	9	20–80	254°/68°N
VNL113	2/6	reversed					246°/66°N
VNL112	5/6	142	–48	9	27	40–80	278°/68°N
VNL111	6/6	192	–59	39	11	40–80	267°/63°N
VNL110	5/6	158	–55	118	7	20–80	260°/58°N
VNL109	6/6	reversed					259°/70°N
VNL108	6/6	172	–44	151	6	30–100	256°/68.5°N
VNL107	6/6	182	–40	181	5	20–80	260°/67°N
VNL106	6/6	213	–66	27	13	50–100	264°/54°N
VNL105	6/6	169	–43	102	7	20–80	255°/67°N
VNL104	6/6	194	–52	48	10	30–100	272°/59°N
VNL103	5/6	172	–50	40	12	30–80	260°/62°N
VNL102	6/6	183	–50	620	3	40–100	267°/60°N
VNL101	5/6	reversed					258°/71°N
VNL10	4/6	196	–35	63	12	80–100	275°/59°N
VNL09	5/5	reversed					268°/54°N
VNL08	6/6	reversed					
VNL07	4/6	170	–46	58	12	40–50	280°/54°N
VNL06	6/6	197	–53	73	8	40–50	276°/59°N
VNL05	6/6	201	–50	245	4	40–50	279°/61°N
VNL04	6/6	reversed					269°/64°N
VNL03	6/6	reversed					265°/64°N
VNL02	6/6	reversed					277°/70°N
VNL99	6/6	185	–42	402	3	30–80	
VNL98	6/6	188	–44	69	8	40–80	270°/57°N
VNL96	6/6	reversed					259°/53.5°N
VNL95	5/6	204	–53	41	12	40–80	271°/54.5°N
VNL92	6/6	161	–67	54	9	40–80	
VNL91	4/6	188	–51	21	15	40–80	264°/65.5°N
VNL90	6/6	173	–59	57	9	30–60	
VNL87	6/6	reversed					
VNL86		unstable					
VNL84	6/6	12	46	29	13	10–30	
VNL82	4/6	356	54	263	6	10–30	259°/58°N
VNL80	6/6	3	41	196	5	40–80	
VNL78	8/8	37	54	149	5	10–30	277°/52°N
VNL76	6/6	7	47	232	4	40–80	265°/50°N
VNL01	6/6	8	50	81	7	40–50	265°/60.5°N
VNL74	6/6	187	–42	48	10	40–80	247.5°/58°NW
VNL70	8/8	reversed					258°/45°N
VNL62	8/8	174	–25	33	10	10–30	261°/45°N
VNL60	4/6	reversed					264°/45.5°N
VNL54		unstable					272.5°/37.5°N
VNL50	5/6	reversed					291°/36°NE

TABLE 4 (continued)

Site	N/n	D, deg	I, deg	k	α_{95}, deg	Demag, mT	Bedding Strike/Dip
VNL44	6/6	194	–35	64	8	40–80	266°/30°N
VNL42	8/8	181	–46	76	6	40–80	
VNL40	7/8	170	–49	162	4	40–80	259°/18°N
VNL37	5/6	182	–42	42	12	40–80	280°/25°N
VNL36	5/6	195	–48	112	7	40–80	
VNL35	3/6	188	–47	74	14	30–80	253°/21°NW
VNL34	6/6	194	–65	61	9	30–80	218°/13.5°NW
VNL33	10/10	209	–64	144	4	40–80	
VNL32	8/8	145	–56	99	6	40–80	
VNL31	6/6	147	–51	45	10	40–80	
VNL30	6/6	166	–46	65	8	40–80	205.5°/21.5°NW
VNL23	8/8	167	–45	50	8	40–80	241.5°/15.5°NW
VNL22	6/6	175	–29	64	8	40–80	237.5°/29.5°NW
VNL21	6/6	170	–39	82	7	40–80	
VNL20	6/6	162	–34	173	5	40–80	233.5°/27.5°NW

See Table 2 notes for definitions of column heads. Site location is 34.30°N latitude, 241.51°E longitude.

in both TL and VNL sections dips steeply to the north, and their structurally uncorrected directions (Figures 7a and 7b) have no meaning when compared with the known average Neogene direction, whereas the structurally corrected directions are consistent with the Neogene geomagnetic field. Moreover, together with the occasional normal polarity sites, the results constitute a successful reversal test in the predominantly reverse Saugus (Figures 7c and 7d).

The characteristic paleomagnetic direction of each specimen was determined from 3 to 6 consecutive levels of progressive AF or thermal demagnetization. When appropriate, site mean directions were calculated in two ways. First, each specimen was assigned equal weight; this usually resulted in data from two specimens per oriented hand sample and six specimens per site (Tables 2–5). Second, we combined the data of specimens from each oriented sample, thereby halving the number of independent vectors. The two methods yielded essentially identical directions. For most sites, estimates of the Fisher [1953] precision parameter (k) increased significantly or hardly changed when the number of

TABLE 5. Horse Flats Section: Site Mean Paleomagnetic Results for Saugus Formation

Site	N/n	D, deg	I, deg	k	α_{95}, deg	Demag, mT	Bedding Strike/Dip
BR1	5/8	341	57	48	11	60–100	267°/17°N
BR2	6/6	354	47	30	12	10–60	
RE4	8/8	18	41	138	5	10–60	286°/42°N
RE3	4/6	normal?			6		154°/52°SW
RE2	4/6	unstable					157°/44°SW
RE1	4/6	unstable					151°/43°SW
NU4	4/6	unstable					283°/28°N
NU3	6/6	18	60	366	4	10–40	291°/28°N
NU2	6/6	normal?					
NU1	4/6	8	48	61	9	10–40	
AN1	4/8	211	–42	610	4	50–100	285°/38°N

See Table 2 notes for definitions of column heads. Site location is 34.29°N latitude, 241.39°E longitude.

TABLE 6. Saugus Formation: Section Mean Summary Data

Site	N	D, deg	I, deg	k	θ_{63}, deg	α_{95}, deg
Magic Mountain Area						
Transmission Line Saugus						
ALL	26	25.7	51.8	26	15.8	5.6
sans (60,59,57)	23	26.4	55.6	45	12.1	4.6
Brunhes	4	12.9	46.6	37	13.3	15.3
Matuyama (all)	22	28.4	52.6	26	15.9	6.2
sans (60,59,57)	19	30.0	57.2	60	10.5	4.4
sans Olduvai	16	31.4	58.8	59	10.5	4.8
Santa Clara River Saugus						
ALL	16	23.0	52.0	57	10.8	5.0
Brunhes	6	15.3	48.1	329	4.5	3.7
Matuyama	10	29.0	54.8	49	11.6	7.0
sans Jaramillo	9	27.9	54.5	45	12.0	7.7
Transmission Line & Santa Clara River Saugus						
ALL	42	24.8	52.0	34	14.0	3.9
sans (60,59,57)	39	25.1	54.3	49	11.6	3.3
Brunhes **	10	14.3	47.5	92	8.5	5.1
Matuyama (all)	32	28.5	53.3	31	14.5	4.6
sans (60,59,57) **	29	29.6	56.4	57	10.7	3.6
Matuyama (reversed)	25	30.0	57.3	53	11.1	4.0
Matuyama (normal)	7	24.8	38.4	24	16.5	12.6
sans (60,59,57)	4	27.5	50.9	154	6.5	7.4
San Fernando Area						
Van Norman Lake Saugus						
ALL	51	358.6	47.1	29	15.0	3.8
Brunhes	5	346.8	32.4	63	10.2	9.7
Matuyama (all)	46	360.5	48.6	32	14.3	3.8
Matuyama (reversed)	40	359.2	48.5	30	14.7	4.2
Olduvai	6	9.7	49.4	65	10.1	8.4
Normal (all)	11	357.8	42.2	26	15.8	9.0
Van Norman Lake & Horse Flats Saugus						
ALL **	57	359.9	47.5	29	14.9	3.5
Normal	16	359.6	45.2	29	15.2	7.0
Brunhes	8	350.8	38.8	30	14.0	10.3
Matuyama (all)	49	1.7	48.8	32	14.4	3.7
Matuyama (reversed)	41	0.0	48.4	29	14.9	4.2
Olduvai	8	10.3	50.5	72	9.5	6.6

N is number of sites; θ_{63} is angular standard deviation in degrees; D and I are average declination (D) and inclination (I) of structurally corrected sites in degrees; k, α_{95} is as described in Table 2. ** indicate the most representative domain mean paleomagnetic directions.

independent measurements was halved, while the radius of the 95% cone of confidence (α_{95}) increased or remained the same. Site mean paleomagnetic directions and the associated statistical parameters (k and α_{95}) for the Saugus and Pacoima formations in the Magic Mountain amusement park area (TL and SCR) and the Van Norman Lake Reservoir-Horse Flats area (VNL and HF) are listed in Tables 2–5. Table 1 shows that 65% of the sampled Saugus sites yielded paleomagnetic directions, using 93% of the specimens from these sites in the analyses.

The angular standard deviations (θ_{63}) of the site mean directions of the Saugus sections vary from 14° to 16° (Table 6), in agreement with other studies from this latitude [McElhinny and Merrill, 1975]. These results suggest that the sampled Saugus sections adequately represent the average behavior of the geomagnetic field and its secular variation.

RESULTS AND DISCUSSION

Magnetostratigraphy of the Saugus Formation near Magic Mountain

Prior to this study the Saugus Formation was known to have been deposited in the Pliocene and Pleistocene, based on Pliohippus and horse teeth collected from the formation [Winterer and Durham, 1962]. Our results show that the Saugus in the Magic Mountain area is predominantly of reverse polarity and is capped by a sequence of normal polarity sites (Figures 3 and 8). The ash bed discovered in the upper normal polarity zone of TL (Figures 3 and 8) has chemical affinities to the Bishop and Friant ashes, and it is not possible to discriminate between them on the basis of geochemistry (work of A. Sarna-Wojcicki as discussed by Levi et al. [1986]). Because the Bishop tephra layer is widespread over the central and western conterminous United States, including southern California, while the Friant ash occurs only rarely, we assume that the ash layer in the TL section is the Bishop tephra (A. Sarna-Wojcicki, personal communications, 1992), which has been recently dated at 0.76 Ma [Izett and Obradovich, 1991; Pringle et al., 1992]. Hence the data indicate that the Saugus in this area was deposited during the Matuyama (reverse) and lower Brunhes (normal) chrons. Therefore the base of Saugus is younger than 2.6 Ma, the age of the Gauss/Matuyama boundary according to the recent revisions of the magnetic polarity time scale, [Johnson, 1982; Shackleton et al., 1990; Hilgen, 1991; Baksi, 1992; Spell and McDougall, 1992; McDougall et al., 1992]. In the SCR section the Brunhes/Matuyama boundary is well constrained between the normal sites SC-6 and SC-57 and reverse site SC-20 (Table 3; Figures 3 and 8). In the TL section it is not clear whether sites TL 100–TL 103 (Table 2; Figures 3 and 8) belong to the Brunhes or the Jaramillo subchron; the latter interpretation is preferred at present, based on the correlation with the SCR section and the 0.76 Ma age of the Bishop ash.

In the Matuyama of the SCR section, we sampled a single normal polarity site (SC 25: Table 3, Figures 3 and 8) about 192 m stratigraphically below the Brunhes/Matuyama boundary. In the Matuyama of the TL section there is a cluster of several normal polarity sites (TL 51–TL 60: Table 2, Figures 3 and 8) about 1010 m below the ash bed. If the normal Matuyama SCR site is assumed to represent the Jaramillo subchron, then the average sedimentation rate between SC 25 and the overlying Brunhes/Matuyama boundary is about 0.8 km/m.y., using the astronomically tuned polarity time scale [Shackleton et al., 1990; Hilgen, 1991]. Similarly, taking the age of the Bishop ash as 0.76 Ma and the normal cluster in the lower TL section as the Olduvai subchron with an average age of 1.86 Ma, one obtains an average sedimentation rate of 0.9 km/m.y. (Figures 8 and 10). The similar average sedimentation rates of the SCR and TL sections, which are separated by just a few kilometers, lends confidence to assigning the normal zones in the SCR and TL sections to the Jaramillo and Olduvai subchrons, respectively.

Subsurface well data in the study area (Yeats et al., submitted manuscript, 1992) suggest that the uppermost exposures in the SCR and TL sections in the Magic Mountain area are

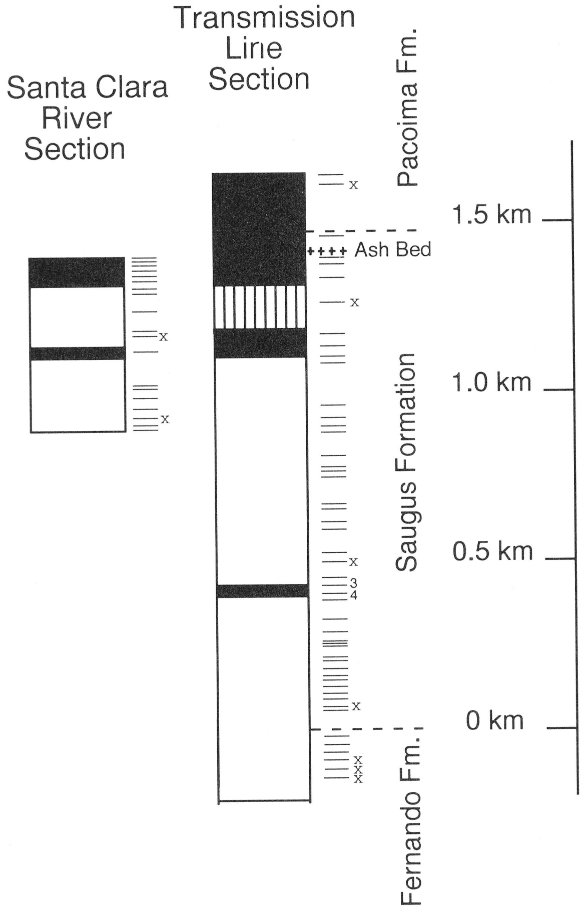

Fig. 8. Magnetic polarity stratigraphy of the Santa Clara River and Transmission Line sections in the Magic Mountain area. Black is normal polarity; white is reverse. Vertical hatches indicate no polarity interpretation. Horizontal dash lines indicate formation boundaries; horizontal dashes to right of polarity column indicate sampling sites. Cross next to site shows that there is no polarity data at the site. (Number adjacent to a site dash indicates the number of sites sampled at this stratigraphic level.) Depth scale on the right hand side shows the stratigraphic thickness.

close to the top of the section in the east Ventura basin. Hence, on the basis of the 0.9 km/m.y. average sedimentation rate, the youngest Saugus (Pacoima) locally was deposited at about 0.6–0.5 Ma. Linear downward extrapolation from the Olduvai subchron, using the same sedimentation rate, the inferred age of the Saugus/Fernando boundary in the TL section is 2.3 Ma. This is consistent with the reverse polarity of the three uppermost Fernando sites at the base of the TL section (Figures 3 and 8). Thus the Saugus in the Magic Mountain area was deposited between about 2.3–0.5 Ma.

The deposition of the continental Saugus sediments was varied and episodic. This is illustrated by the presence of numerous conglomerates and layers of coarse-grained sandstone. The paleomagnetic results further suggest that some of the fine-grained overbank deposits can accumulate at prodigious rates. For example, in the TL section about 60 m of section, represented by sites TL 14, TL 16, TL 19, and TL 21, recorded an essentially identical, yet distinct, paleomagnetic direction (Table 2). On the basis of archeomagnetic data about rates of secular variation [e.g., Merrill and McElhinny, 1983], these units were probably deposited in less than 1000 years, in contrast to more than 50,000 years calculated from the average sedimentation rate. As another illustration, sites TL 57, TL 59, and TL 60, which represent 20–30 m of section, recorded the same intermediate direction (Table 2), suggesting that they probably represent less than a few hundred years. (Hence these fine-grained overbank deposits can be considered the sedimentary equivalents of lavas in recording instantaneous paleomagnetic directions.) These results further suggest that significant intervals of the Saugus and Pacoima formations between 2.3 and 0.5 Ma might be represented by disconformities, due in part to nondeposition as well as scouring and erosion of the section by a high-energy flow regime.

In the TL section, the inferred Saugus/Pacoima boundary (J. A. Treiman, written communications, 1991) is in the Brunhes, just above the ash locality, with an extrapolated age estimate of about 0.7–0.6 Ma for the boundary. In the SCR section, the Saugus/Pacoima boundary as mapped by Weber [1982] is also in the Brunhes chron (Figure 3).

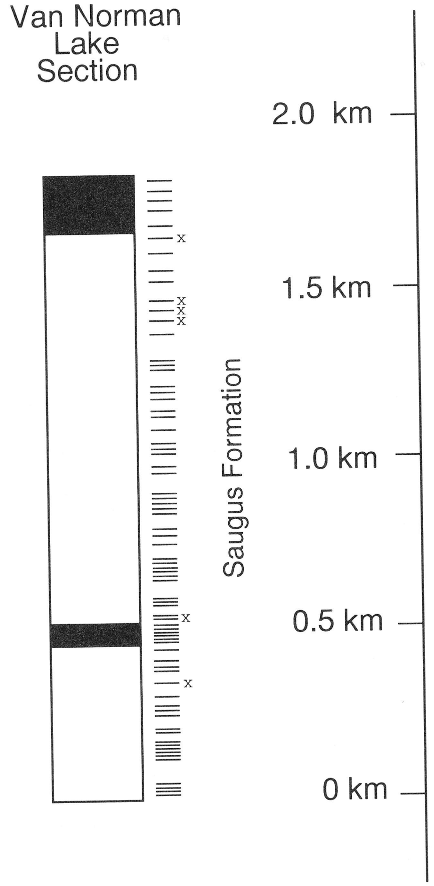

Fig. 9. Magnetic polarity stratigraphy of the Van Norman Lake section in the northwest San Fernando Valley. Black is normal polarity; white is reverse. Horizontal dashes to right of polarity column represent sampling sites. Cross next to site shows that there is no polarity data at the site. Depth scale on the right hand side shows the stratigraphic thickness.

Magnetostratigraphy of the Van Norman Lake-Horse Flats Area

The VNL Saugus section, along and just west of Van Norman Lake (Figures 4 and 9), is approximately 1.9 km thick. The uppermost five sites are normal, while the underlying reverse section includes a zone of six normal sites in the lower Sunshine Ranch member of Saugus, representing 60–70 m of section (Table 4; Figures 4 and 9). By analogy with the reference section near Magic Mountain, we conclude that the VNL section was deposited mostly during the Matuyama, and the normal sites at the top of the section belong to the Brunhes chron (Figure 10). From the position and extent of the normal sites in the Sunshine Ranch member, we infer that they were probably deposited during the Olduvai subchron, 1.77–1.95 Ma [Hilgen, 1991]. The average sedimentation rate of the VNL section, using the estimated stratigraphic positions of the Brunhes/Matuyama boundary and the Olduvai subchron, is 1.1 km/m.y., based on Shackleton et al.'s [1990] and Hilgen's [1991] polarity time scale. Uncertainties in identifying the correct stratigraphic position of reversals lead to estimated uncertainties in the average sedimentation rates on the order of ± 0.1 km/MY. These results suggest that the youngest Saugus sediment exposed in the VNL section has an age of about 0.7–0.6 Ma. However, the top of the VNL section is about 200 m south of the inferred position of the Mission Hills syncline, indicating that about 100–150 m of section might be missing from the top of the VNL section. Introducing the "missing" 100–150 m to the VNL section would suggest that Saugus deposition in the Van Norman Lake area ended circa 0.6–0.5 Ma. The base of Saugus in the VNL section has an extrapolated age of about 2.3 Ma, very similar to the age of the Saugus/Fernando boundary of the TL section in the Magic Mountain area, but the average sedimentation rate in the VNL section is about 20% higher.

On the basis of the results in the VNL section, the cluster of normal sites along Nugent Street, about 2 km west of the VNL section (middle of Figure 4; Table 5), would seem to correlate

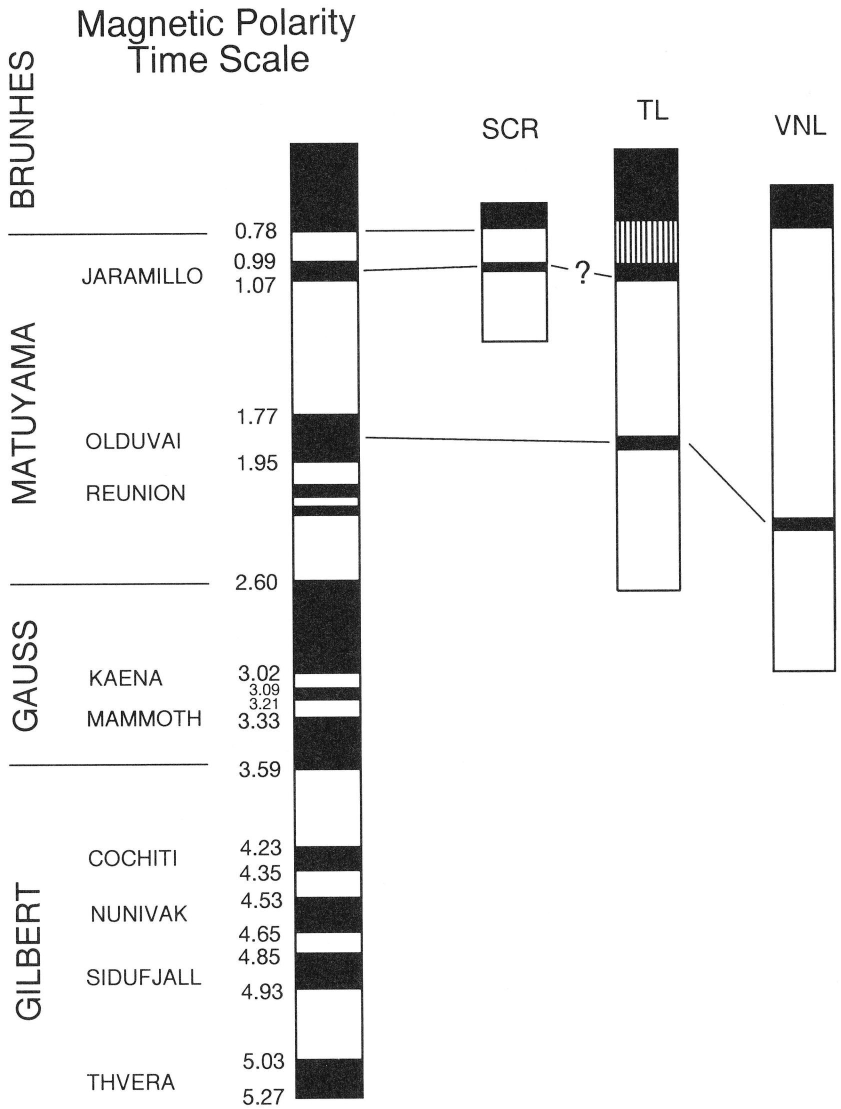

Fig. 10. Interpretation of the polarity stratigraphy in terms of the magnetic polarity time scale of Hilgen [1991] and Shackleton et al. [1990].

with the Olduvai subchron. The normal sites at Reseda Boulevard and Braemore Road on the south side of Horse Flats (left part of Figure 4) represent the Brunhes chron, and because they are from the upper Saugus member, they must be younger than the Brunhes sites in the VNL section.

Timing of Uplift of the Santa Susana Mountains

The upper Saugus of the Van Norman Lake-Horse Flats area is distinguished from the underlying sediments in being comprised of locally derived [Saul, 1979, p. 9] "sandstone concretions and ever more angular fragments of porcelaneous shale, rocks common in the Towsley and Modelo Formations now exposed to the north in the Santa Susana Mountains. The base of the upper member is drawn where the coarse clastic beds are almost exclusively sandstone and shale fragments. The remaining small proportion of cobbles of igneous and metamorphic rocks probably were reworked from the new source area." Because the sediment of the middle and Sunshine Ranch members of Saugus are considered to originate predominantly from more remote source areas north and northeast in the Soledad basin, the more local source of the upper Saugus is taken as evidence for the beginning of uplift of the Santa Susana Mountains. This suggests that the initiation of uplift of the Santa Susana Mountains has occurred since 0.7–0.6 Ma (Figure 11), the extrapolated age of the top of the VNL section. This age is very similar to the independently estimated age of the Saugus/Pacoima boundary in the TL section, which is also characterized by a change from remote to predominantly locally derived clasts from the Saugus Formation itself. Because this uplift was produced by the initiation of upward ramping on the Santa Susana fault, determining the displacements of the base of the Saugus Formation on both sides of the fault should permit the calculation of late Quaternary slip rate on this fault (G. Huftile and R. S. Yeats, manuscript in preparation, 1992).

Paleomagnetic Directions

In the Magic Mountain area, 42 of the 70 sampled sites yielded paleomagnetic directions, and, for these sites, more than 90% of the specimens were used in calculating the mean directions (Table 1). The mean paleomagnetic directions from the TL and SCR sections are statistically indistinguishable, and therefore they are treated together (Table 6). In calculating the mean direction we exclude the results from sites TL 57, TL 59, and TL 60, because the paleomagnetic directions of these sites deviate from the mean of all 42 sites by more than twice the angular standard deviation. Sites TL 57, TL 59, and TL 60 are interpreted to have acquired their remanence during the polarity transition from the normal Olduvai to the overlying reverse Matuyama chron. The average direction for 39 sites is $D = 25°$, $I = 54°$, $\alpha_{95} = 3°$ (Table 6). The mean inclination is identical to the expected geocentric axial dipole inclination at this site, indicating that the fine-grained Saugus sediments in this area recorded the paleomagnetic field with no discernable inclination shallowing. The average declination of the Saugus Matuyama sites (N=29) in this area shows 30° clockwise rotation since about 2.3 Ma. The 10 Brunhes sites are rotated 14° clockwise (Figure 12; Table 6). If the rotation of the Magic Mountain area were progressive since sometime in the Matuyama, then the data would suggest that the rotation began prior to the uplift of the Santa Susana Mountains. On the other hand, if the progressive appearance of the rotation were a rock magnetic artifact, due to incomplete removal of a secondary overprint component, then about 25° of clockwise rotation has taken place since sometime in the Brunhes, accompanying the uplift of the Santa Susana Mountains.

In the Van Norman Lake-Horse Flats area south of the Santa Susana fault more than two thirds of the sampled sites yielded paleomagnetic directions (Table 1). The mean direction for 57 sites is $D = 360°$, $I = 48°$, $\alpha_{95} = 4°$, showing no

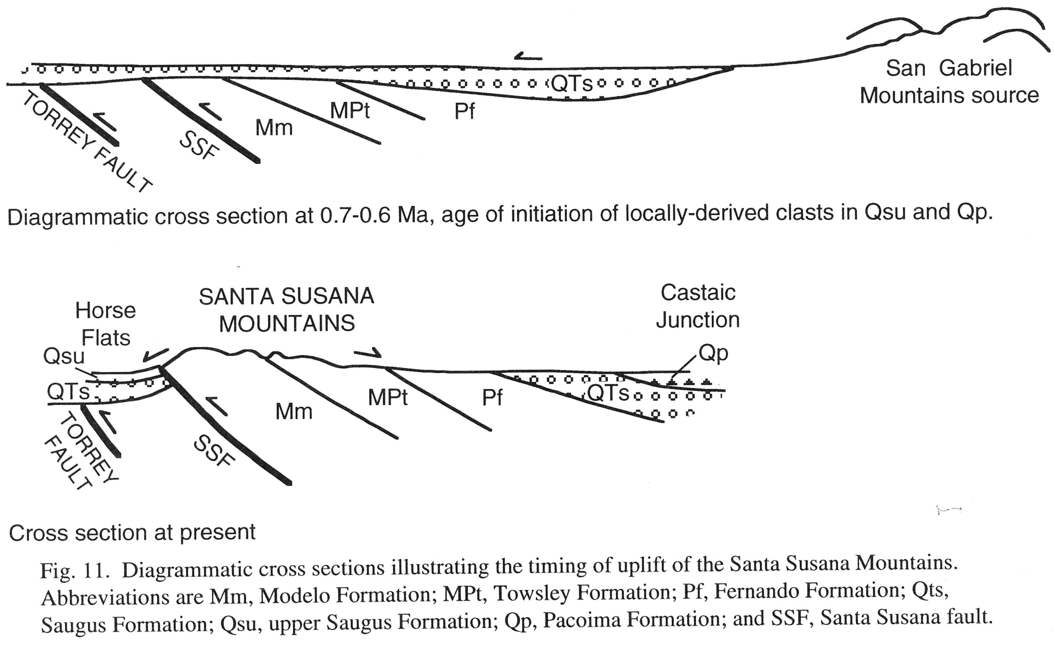

Fig. 11. Diagrammatic cross sections illustrating the timing of uplift of the Santa Susana Mountains. Abbreviations are Mm, Modelo Formation; MPt, Towsley Formation; Pf, Fernando Formation; Qts, Saugus Formation; Qsu, upper Saugus Formation; Qp, Pacoima Formation; and SSF, Santa Susana fault.

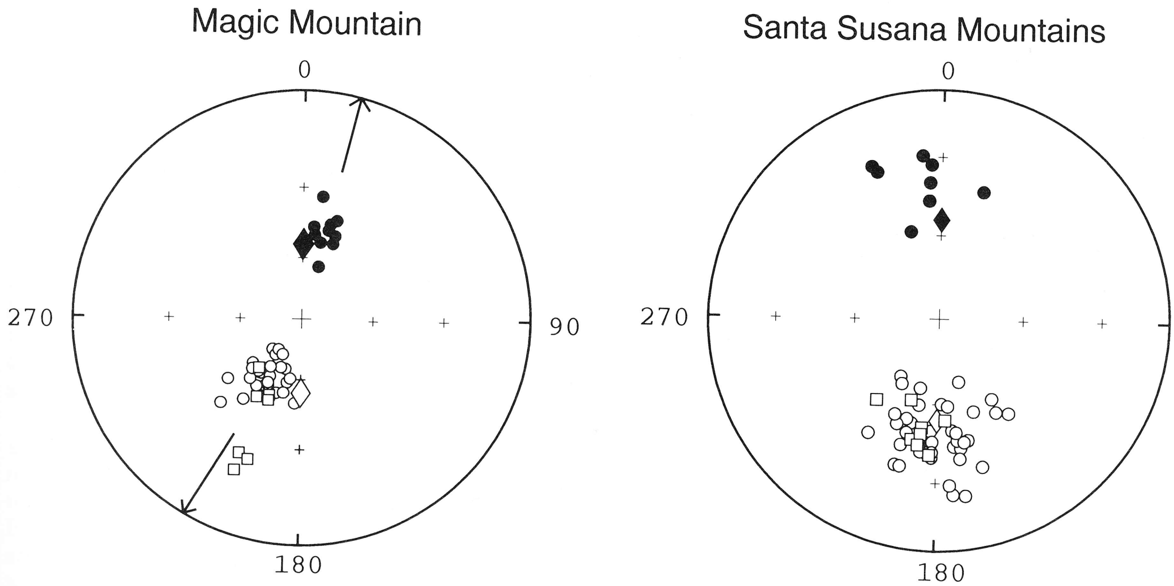

Fig. 12. Site mean, structurally corrected directions for the Magic Mountain and Santa Susana Mountains areas. Diamonds represent the Plio-Pleistocene geocentric axial dipole. Solid circles are lower hemisphere Brunhes directions; open circles, upper hemisphere directions of Matuyama sites; open squares represent Olduvai and Jaramillo sites, with directions inverted to reverse polarity. The arrows to the perimeter of the upper stereogram indicate the average declinations of the Matuyama and Brunhes sites.

rotation and inclination shallowing of about 6° (Figure 12; Table 6).

The two study areas represent neighboring domains, each of a few square kilometers (Figure 2). One is rotated; the other is not. The average clockwise rotation is consistent with the gross dextral shearing interaction between the North American and Pacific plates [e.g., Jackson and Molnar, 1990], while the specific deformation of each domain is probably determined by its geometry and interactions with adjacent domains along the boundaries. It is not surprising that in such a tectonically active area small domains can exhibit high rates of rotations.

CONCLUSIONS

1. Magnetic stratigraphy of the fine-grained Saugus and Pacoima strata and the discovery of the 0.76 Ma Bishop ash show that the Saugus and Pacoima formations both north and south of the Santa Susana fault were deposited from about 2.3 to 0.5 Ma.

2. The average Saugus sedimentation rate south of the Santa Susana fault west and adjacent to the Van Norman Lake Reservoir is 1.1 km/m.y., more than 20% higher than north of the fault in the Magic Mountain area, where the average sedimentation rate is about 0.9 km/m.y.

3. Magnetostratigraphic dating of the Saugus/Pacoima boundary in the Magic Mountain area and the Saugus/upper Saugus boundary at Horse Flats, above which the predominant clasts are locally derived from units now exposed in the Santa Susana Mountains, suggests that the initiation of uplift of the Santa Susana Mountains occurred about 0.7–0.6 Ma.

4. Paleomagnetic directions of the Saugus Formation in the Magic Mountain domain north of the Santa Susana fault, bordered to the north and northeast by the Holser and San Gabriel faults, respectively, suggest that this domain has rotated 30° clockwise since 2.3 Ma, while the Saugus of the Van Norman Lake domain south of the Santa Susana fault shows no rotation during this time interval.

Acknowledgments. We thank the Newhall Land and Farming Company for permission to sample on their properties in the Magic Mountain area and J. A. Treiman for his advice and for providing his unpublished field notes of the TL and SCR sections. L. T. Stitt participated in the field work that discovered the ash bed in the TL section and that was subsequently chemically analyzed by A. Sarna-Wojcicki. Dennis Schultz assisted in the field and did the paleomagnetic measurements. This study was supported by the U.S. Geological Survey: NEHRP contract 14-08-0001-G1353. J. A. Treiman and P. L. Ehlig provided very useful reviews of the manuscript.

REFERENCES

Baksi, A.K., V. Hsu, M.O. McWilliams, and E. Farrar, $^{40}Ar/^{39}Ar$ dating of the Brunhes Matuyama geomagnetic field reversal, *Science*, *256*, 356–357, 1992.

Barrows, A.G., J.E. Kahle, R.B. Saul, and F.H. Weber, Jr., Geologic map of the San Fernando earthquake area 1:18,000, *Calif. Div. Mines Geol., Bull. 196*, 1975.

Ehlig, P.L., Geologic framework of the San Gabriel Mountains, *Calif. Div. Mines Geol., Bull. 196*, 7–18, 1975.

Fisher, R., Dispersion on a sphere, *Proc. R. Soc. London Ser. A*, *217*, 295–305, 1953.

Hilgen, F.J., Extension of the astronomically calibrated (polarity) time scale to the Miocene/Pliocene boundary, *Earth Planet. Sci. Lett.*, *107*, 349–366, 1991.

Izett, G., and J. Obradovich, Dating of the Matuyama-Brunhes boundary based on $^{40}Ar/^{39}Ar$ age of the Bishop Tuff and Cerro San Luis rhyolite, *Geol. Soc. Am. Abstracts with Programs*, *23*, A106, 1991.

Jackson, J., and P. Molnar, Active faulting and block rotations in the Western Transverse Ranges, California, *J. Geophys. Res.*, *95*, 22,073–22,087, 1990.

Jennings, C.W., compiler, Geologic map of California, scale 1:750,000, 1975.

Jennings, C.W., and R.G. Strand, Geologic map of California, Los Angeles sheet, scale 1:250,000, Calif. Div. of Mines and Geol., Sacramento, 1969.

Johnson, R.G., Brunhes-Matuyama magnetic reversal dated at 790,000 yr B.P. by marine-astronomical correlations, *Quat. Res.*, *17*, 135–147, 1982.

Kew, W.S.W., Geology and oil resources of a part of Los Angeles and Ventura counties, California, *U.S. Geol. Surv. Bull.*, *753*, 202 pp., 1924.

Lant, K.J., Structure of the Aliso Canyon area, eastern Ventura basin, California, M.S. thesis, 79 pp., Ohio Univ., Athens, 1977.

Lee, W.H.K., R.F. Yerkes, and M. Simirenko, Recent earthquake activity and focal mechanisms in the western Transverse Ranges, California, *U.S. Geol. Surv. Circ. 799-A*, 1–26, 1979.

Levi, S., D.L. Schultz, R.S. Yeats, L.T. Stitt, and A.M. Sarna-Wojcicki, Magnetostratigraphy and paleomagnetism of the Saugus Formation, near Castaic, Los Angeles County, California, in *Field Trip Guidebook and Volume on Neotectonics and Faulting in Southern California and Baja California*, edited by P.E. Ehlig, pp. 103–108, Cordilleran Section, Geological Society of America, Los Angeles, Calif., 1986.

McDougall, I., F.H. Brown, T.E. Cerling, and J.W. Hillhouse, A reappraisal of the geomagnetic polarity time scale to 4 Ma using data from the Turkana Basin, east Africa, *Geophys. Res. Lett.*, *19*, 2349–2352, 1992.

McElhinny, M.W., and R.T. Merrill, Geomagnetic secular variation over the past 5 m.y., *Rev. Geophys. Space Phys.*, *13*, 687–708, 1975.

Merrill, R.T. and M.W. McElhinny, The Earth's Magnetic Field: Its History, Origin and Planetary Perspective, 401 pp., Academic, San Diego, Calif., 1983.

Oakeshott, G.B., Geology and mineral deposits of San Fernando quadrangle, Los Angeles County, California, *Calif. Div. Mines*, *Bull. 172*, 147 pp., 1958.

Pringle, M.S., M. McWilliams, B.F. Houghton, M.A. Lanphere, and C.N.J. wilson, $^{40}Ar/^{39}Ar$ dating of Quaternary feldspar: Examples from Taupo Volcanic Zone, New Zealand, *Geology*, *20*, 531–534, 1992.

Sarna-Wojcicki, A.M., K.R. Lajoie, C.E. Meyer, D.P. Adam and H.J. Rieck, Tephrochronologic correlation of upper Neogene sediments along the Pacific margin, conterminous United States, in *The Geology of North America*, *vol. K-2*, *Quaternary Nonglacial Geology: Conterminous U.S.*, pp. 117–140, Geological Society of America, Boulder, Colo., 1991.

Saul, R.B., Geology of the southeast slope of the Santa Susana Mountains and geologic effects of the San Fernando earthquake, *Calif. Div. Mines Geol.*, *Bull. 196*, 53–70, 1975.

Saul, R.B., Geology of the S.E. 1/4 Oat Mountain Quadrangle, Los Angeles County, California, map sheet 30, Calif. Div. of Mines and Geol., Sacramento, 1979.

Shackleton, N.J., A. Berger, and W.R. Peltier, An alternative astronomical calibration of the lower Pleistocene timescale based on ODP Site 677, *Trans. R. Soc. Edinburgh Earth Sci.*, *81*, 251–161, 1990.

Spell, T.L., and I. McDougall, Revisions to the age of the Brunhes-Matuyama boundary and the Pleistocene geomagnetic polarity timescale, *Geophys. Res. Lett.*, *19*, 1181–1184, 1992.

Treiman, J.A., Geological hazards in the west half of the Newhall quadrangle, Los Angeles County, California, *Calif. Div. Mines Geol.*, *Open File Rept. 86-6 LA*, 1986.

Weber, F.H., Jr., Geology and geomorphology along the San Gabriel fault zone, Los Angeles and Ventura counties, California, *Calif. Div. Mines Geol.*, *Open File Rept. 82-2 LA*, 1982.

Winterer, E.L., and D.L. Durham, Geology of southeastern Ventura basin, Los Angeles County, California. *U.S. Geol. Surv. Prof. Pap. 334-H*, 275–366, 1962.

Yeats, R.S., Stratigraphy and paleogeography of the Santa Susana fault zone, Transverse Ranges, California, in *Cenozoic paleogeography of the western United States*, edited by J.M. Armentrout, M.R. Cole, and H. Ter Best, pp. 191–204, Pacific Section, Soc. Econ. Paleontologists and Mineralogists Cenozoic Paleography Symposium, 1979.

Yeats, R.S., Late Cenozoic structure of the Santa Susana fault zone, *U.S. Geol. Surv. Prof. Pap. 1339*, 137–160, 1 plate, 1987.

Yeats, R.S., W.H.K. Lee, and R.F. Yerkes, Geology and seismicity of the eastern Red Mountain fault, Ventura County, *U.S. Geol. Surv. Prof. Pap. 1339*, 161–167, 1987.

Yerkes, R.F., and W.H.K. Lee, Maps showing faults and fault activity and epicenters, focal depths and focal mechanisms for 1970–75 earthquakes, Western Transverse Ranges, California, 2 sheets, U.S. Geol. Surv. Misc. Field Stud. Map MF-1032, scale 1:250,000, 1979.

S. Levi, College of Oceanic & Atmospheric Sciences, Oregon State University, Ocean Admin Bldg 104, Corvallis, OR 97331-5503.

R.S. Yeats, Department of Geosciences, Oregon State University, Wilkinson Hall 104, Corvallis, OR 97331-5506.

(Received July 31, 1992;
revised January 11, 1993;
accepted January 18, 1993.)